Published in final edited form as:
Dev Biol. 2007 May 1; 305(1): 172–186.

Identification of Oscillatory Genes in Somitogenesis from Functional Genomic Analysis of a Human Mesenchymal Stem Cell Model

Dilusha A. William[1,2,*], **Biagio Saitta**[3,*], **Joshua D. Gibson**[1,4], **Jeremy Traas**[1], **Vladimir Markov**[3], **Dorian M. Gonzalez**[1], **William Sewell**[4], **Douglas M. Anderson**[4], **Stephen C. Pratt**[4], **Eric F. Rappaport**[1], and **Kenro Kusumi**[1,2,4,5,†]

1 *Divisions of Human Genetics and Orthopaedic Surgery, Children's Hospital of Philadelphia, 3615 Civic Center Blvd., Philadelphia, PA 19104*

2 *Departments of Pediatrics and Cell & Developmental Biology, University of Pennsylvania School of Medicine, Philadelphia, PA*

3 *Coriell Institute for Medical Research, 403 Haddon Avenue, Camden, NJ 08103*

4 *School of Life Sciences, Arizona State University, PO Box 874501, Tempe, AZ 85287*

5 *Department of Basic Medical Sciences, University of Arizona College of Medicine-Phoenix, 550 E. Van Buren St., Phoenix, AZ 85004*

Abstract

During somitogenesis, oscillatory expression of genes in the notch and wnt signaling pathways plays a key role in regulating segmentation. These oscillations in expression levels are elements of a species-specific developmental mechanism. To date, the periodicity and components of the human clock remain unstudied. Here we show that a human mesenchymal stem/stromal cell (MSC) model can be induced to display oscillatory gene expression, including known cycling genes such as *HES1* that displayed a period of 5 hours. We also observed cycling of *Hes1* expression in mouse C2C12 myoblasts with a period of 2 hours, consistent with previous *in vitro* and embryonic studies. Furthermore, we used microarray and quantitative PCR (Q-PCR) analysis to identify additional genes that display oscillatory expression both *in vitro* and in mouse embryos. We confirmed oscillatory expression of the notch pathway gene *Maml3* and the wnt pathway gene *Nkd2* by whole mount *in situ* hybridization analysis and Q-PCR. Expression patterns of these genes were disrupted in *Wnt3a*^{tm1Amc} mutants but not in *Dll3*^{pu} mutants. Our results demonstrate that human and mouse *in vitro* models can recapitulate oscillatory expression observed *in embryo* and that a number of genes in multiple developmental pathways display dynamic expression *in vitro*.

Keywords

oscillatory; somite; somitogenesis; segmentation; mesenchymal; stem cell; microarray; notch pathway; wnt pathway; cycling; Fourier

*Authors contributed equally
†Correspondence should be sent to: Kenro Kusumi School of Life Sciences Arizona State University PO Box 874501 Tempe, AZ 85287-4501 Email: kenro@asu.edu Tel. (480) 727-8993 FAX (480) 965-6899

Introduction

During somitogenesis, segments are repeatedly formed at the rostral end of the presomitic mesoderm (PSM) to generate the vertebrate body axis (Tam & Trainor, 1994;Keynes & Stern, 1988). This segmentation process is dependent on a molecular clock mechanism involving transient waves of synchronized gene expression within the PSM (Aulehla & Hermann, 2004; Dubrulle & Pourquie, 2004b; Iulianella et al., 2003;Sato et al., 2002). A number of gene pathways have been shown to coordinately regulate this process. The notch pathway genes *Lfng*, *Hes7*, *Hes1*, *Hes5*, *Hey1* and *Hey2* have been shown to display "cycling" expression, i.e., expression that oscillates rostro-caudally within the PSM each somite cycle (Aulehla & Johnson, 1999; Bessho et al., 2001a; Bessho et al., 2001b; Barrantes et al., 1999;Dunwoodie et al., 2002;Forsberg et al., 1998;Jiang et al., 2000;Jouve et al., 2000;Leimeister et al., 1999;Leimeister et al., 2000a;McGrew et al., 1998;Nakagawa et al., 1999). For *Hes7*, this oscillation is regulated by a negative autoregulatory feedback loop, with the clock rate dependent on the half-life of mRNA and protein (Hirata et al., 2004). For *Lfng*, oscillatory expression is dependent on *de novo* protein synthesis and is also sensitive to disruptions in notch signaling (Kusumi et al., 2004;McGrew et al., 1998). The wnt pathway genes *Axin2* and *Nkd1* and the transcription factor snail (*Snai1*) also have been shown to display cycling expression, with disruptions in the wnt pathway affecting the cycling of notch pathway genes (Aulehla et al., 2003;Dale et al., 2006). The periodic localized expression of *Axin2* within the PSM is out of phase with that of notch pathway cycling genes, suggesting that the oscillatory mechanism is complex. Other genes such as *Mesp2* have been observed to display stage-specific expression, with oscillatory variation in length of expression stripes within the PSM (Saga et al., 1997;Takahashi et al., 2000).

Oscillatory expression can also be induced in cell culture, raising the possibility of modeling complex interactions of the segmentation clock *in vitro*. *Hes1* oscillations have been observed in synchronized mouse myoblasts (C2C12) with the same 2-hour periodicity observed in mouse embryos (Hirata et al., 2002). In addition, *Hes1* oscillations were induced in fibroblasts (C3H10T1/2), neuroblastoma cells (PC12), and teratocarcinoma cells (P9; Hirata et al., 2002). No cell culture model using human cells has been reported. An *in vitro* model of the segmentation clock would be particularly valuable to study the etiology of human somitogenesis defects, since embryological studies are not possible. Mutations in the human notch pathway genes *DLL3* and *LFNG* have been shown to cause severe vertebral birth defect syndromes (Bulman et al., 2000;Sparrow et al., 2006). The rate of the segmentation clock is highly species-specific and divergent, with periods ranging from an average of 30 minutes in zebrafish to 90 minutes in the chick and 2 hours in the mouse (Saga & Takeda, 2001). The rate in human is not known, although 2-4 somites are estimated to be formed per day based on a collection of human embryos at different stages (Sadler, 2000), which is much slower than any previously studied clock-rate. Furthermore, microarray-based approaches could be used to identify additional oscillatory genes and downstream targets in the segmentation clock.

Towards these goals, we used a mesenchymal stem/stromal cell (MSC) population derived from umbilical cord blood (UCB1; Markov et al., in press) that displays a differentiation profile similar to the cells that populate the presomitic mesoderm and has been characterized by microarray analysis. MSCs are fibroblast-like cells that are self-renewing and can differentiate into mesoderm-derived tissues, including cartilage, bone, fat and muscle (Baksh et al., 2004;Caplan, 1994;Deans & Moseley, 2000;Javazon et al., 2004;Roufosse et al., 2004). We synchronized UCB1 cells and collected samples at regular intervals over 24 hours to examine gene expression by Affymetrix microarrays and Q-PCR. We used Fourier analysis to identify oscillatory gene candidates. For top candidates, we examined expression of mouse homologues in somitogenesis-stage mouse embryos.

MATERIALS AND METHODS

Cell culture, synchronization, and RNA extraction

Mouse C2C12 myoblast cells (Lot # 3258903) were purchased from ATCC, (www.atcc.org) and grown according to manufacturer's protocol.

Human umbilical cord-blood mesenchymal stem cell population UCB1 (Markov et al., in press) were maintained in culture medium (DMEM high glucose with 10% fetal bovine serum, FBS), which was replaced twice weekly. The cells were then seeded at a density of 6,000-10,000 cells/cm^2 and expanded in DMEM high glucose with 10% FBS. After 5-7 days of incubation at 37°C in a humidified atmosphere containing 5% carbon dioxide, cells were detached with 0.05% trypsin for 2 minutes at confluency. Cells were assayed at passage 10.

Cells were synchronized using low serum treatment, which has been described previously for *Hes1* (Hirata et al., 2002). Cell culture synchronization is required to assay oscillatory expression levels, otherwise the oscillations of individual cells would be out of phase and cancel one another. Synchronized cells will gradually desynchronize, leading to diminished oscillatory amplitude. Briefly, synchronization was carried out as follows: T-25 cm flasks (for UCB1 and C2C12) were set up in parallel. These cells were grown to 90% confluence in DMEM supplemented with 5% FBS (for the C2C12) and 10% FBS (UCB-MSC), then incubated in DMEM with only 0.2% FBS for 24 hours, and returned to DMEM supplemented with FBS. For human UCB1, samples were collected at 30 min. intervals from 0 to 8 hours, and then at 1 hour intervals from 9 to 24 hours. In addition, an unsynchronized cell culture was sampled. For mouse C2C12 cells, samples were collected every 30 min. for 8 hours. Total RNA was isolated from cells in culture using the RNeasy Mini Kit (Qiagen).

Microarray analysis to identify oscillatory gene candidates

Microarray analysis was carried out using the Affymetrix mouse MOE430v2 and human HG-U133A and B array sets, following manufacturer's protocol. In brief, double stranded cDNA was synthesized from 5 μg of total RNA using a SuperScript RT II Kit (Invitrogen). Then, biotin labeled cRNA targets were prepared from double stranded cDNA using a Bioarray HighYield RNA Transcript Labeling Kit (Enzo). After hybridization and washes, arrays were scanned and analyzed both for genes that were present and for changes in expression level across time using Microarray Analysis Suite (MAS) 5.0 using default settings ($t = 0.015$, $a_1 = 0.05$, $a_2 = 0.065$) and a median intensity value = 150. To minimize global variation in detection between arrays due to technical error, we used quantile normalization by the Robust Multichip Average (RMA) method to minimize technical variation (Bioconductor 1.5 module; www.bioconductor.org) of the R statistical suite version 1.9.1 (www.r-project.org) and RMA module of Genespring GX 7.3 (Silicon Genetics).

To screen probes for oscillatory expression patterns, we applied a fast Fourier transform to each probe's time series of expression levels, using the ‘spectrum’ command in R. The resulting periodogram measured the strength of oscillatory components with different periods, ranging from one to nine hours. We reasoned that oscillatory genes associated with somitogenesis would have relatively long periods, and that shorter-period components would represent noise or unrelated dynamic expression patterns. Hence, for each probe we determined the peak power among components with periods greater than 3 hours, and we compared this value to the corresponding peak among components with periods less than 1.7 hours. We selected as candidates those probes for which the long-period peak exceeded the 99.95% confidence interval of the short-period peak. This yielded a list of 4,491 probes that we further refined to 1,409 candidates by removing those that were called absent by Affymetrix MAS 5.0 in a majority of samples and by visual inspection of time series to eliminate probes lacking obvious

long-period oscillations. To supplement this broad screen, we also inspected members of known segmentation clock pathways and homologues of somite development genes, even if they did not emerge from the Fourier analysis. From these lists we sampled 20 genes for detailed investigation, focusing on those with particularly robust oscillatory expression patterns, reports of expression in early embryonic development, or relatedness to genes known to be involved in somitogenesis.

Quantitative PCR validation of gene expression changes

We used quantitative PCR to confirm the expression of candidate genes. For Real-time™ quantitative PCR analysis (Applied Biosystems), 1.0 μg of UCB-MSC or C2C12 double stranded cDNA was used. Assays tested on human MSCs are shown in Table 1. *GAPDH/ Gapdh* was used to normalize Q-PCR results, and the assays used were Hs99999905_m1 (*GAPDH*) and Mm99999915_g1 (*Gapdh*). Beta-actin was also used to examine expression as a control, and assays used were Hs99999903_m1 (*ACTB*) and Mm00607939_s1 (*Actb*). Cycling conditions used for the Taqman Real-time PCR were: 95°C 10 minutes followed by 40 cycles of 95°C 15 seconds and 60°C 1 minute.

Analysis of candidate gene expression in mouse embryos by in situ hybridization

Mouse homologues of candidate oscillatory genes were identified for analysis of embryonic expression (Unigene, NCBI). *In situ* hybridization probes were generated from the IMAGE cDNA clones: *Amotl2* (5709126), *Axud1* (5011401), *Bhlhb2* (6530971), *C14orf43* (5026104), *Ctgf* (5323271), *Cyr61* (2616375), *Glcci1* (4505211), *Hhex* (5124938), *Id1* (949768), *Id2* (6515664), *Klf10* (3155247), *Maml3* (6506044), *Nkd2* (6314370), *Nuak1* (3662840), *Rasa4* (5361403), *Slc2a3* (6331145), *Smurf2* (3469700), *Snai2* (1885616, 466831), *Tcf7l2* (5702449), *Znf537* (2865773).

RNA probes for *in situ* hybridization were synthesized using digoxigenin-labeled-UTP (Roche) with MAXIscript™ *in vitro* transcription kits (Ambion), and purified using MC Ultrafree filtration units (Millipore). Whole mount *in situ* hybridization with digoxigenin labeled probes was carried out as described previously (Harrison et al., 1995; Wilkinson et al., 1992), and visualized with NBT/BCIP reagents (Roche) with minor modifications. Expression was examined in mouse embryos in early and mid-somitogenesis (8.5 to 10.5 *days post coitum*, dpc). To compare expression of two genes within the PSM, we bisected the caudal paraxial mesoderm of fixed 9.5 dpc embryos into axial halves, prior to *in situ* hybridization. To confirm cycling gene expression, we bisected the caudal paraxial mesoderm of 9.5 dpc embryos into axial halves, fixing one half while culturing the remaining half for 60 min. in DMEM/50% FBS (Kusumi et al., 2004; adapted from Forsberg et al., 1998) or for 2 and 3 hours. *Dll3*^{pu} cross embryos were genotyped as described previously (Kusumi et al., 1998). *Wnt3a*^{tm1Amc} cross embryos were genotyped by PCR with the following primers: detection of targeted allele Wnt3a12: 5' ACT ACA ACC CTC CTC ACC TG 3' and Wnt3aNeo: 5' TGG CTA CCC GTG ATA TTG CT 3'; detection of wild-type allele Wnt3a12: 5' ACT ACA ACC CTC CTC ACC TG 3'and Wnt3aE3: 5' GTT GTG ACG GTT CAT GGC AG 3'. For *in situ* hybridization studies, mutant embryos were assayed concurrently with wild-type littermate embryos to minimize experimental variation.

Cryosections were performed as previously described (Anderson et al., 2006). Briefly, tissues were embedded in a solution of 15% sucrose and 7.5% gelatin in PBS and frozen in liquid nitrogen. The frozen block was sectioned on a cryostat at a thickness of 25 μm and collected on gelatin-subbed slides. The slides were incubated in warm PBS to remove the gelatin and then dehydrated in an ethanol series and mounted with coverslips.

Accession numbers

Data sets from Affymetrix microarray analysis of UCB1 human mesenchymal stem cells (HG-U133A and HG-U133B) and C2C12 mouse myoblasts (MOE430v2) are deposited at the Gene Expression Omnibus (www.ncbi.nlm.nih.gov/geo) with accession numbers GSE7015 (UCB1) and GSE7012 (C2C12).

Results

Hes1 has been shown to display oscillatory expression in synchronized mouse C2C12 cell culture with a 2 hour periodicity (Hirata et al., 2002). We confirmed that *Hes1* displays oscillatory expression with a periodicity of 2 hours in synchronized mouse C2C12 cells assayed over a period of 8 hours using Affymetrix MOE430v2 arrays and confirmed by quantitative PCR (Fig. 1A,B). To develop a human *in vitro* model of the segmentation clock, we used UCB1 mesenchymal stem cells, which display a differentiation profile similar to presomitic mesoderm (Markov et al., in press). Synchronized human UCB1 cells were assayed over a period of 12 hours by Affymetrix HG-U133A and B arrays. We identified two peaks of human *HES1* expression separated by an approximately 5 hour interval (Fig. 1C). To confirm the periodicity over a longer interval, we used quantitative PCR to assay expression over 24 hours (Fig. 1D) and confirmed a *HES1* periodicity of approximately 5 hours. *HES1* expression showed variable amplitude, consistent with reports of similar variation in cell culture (Masamizu et al., 2006). This is the first demonstration of oscillatory expression of a segmentation clock gene in human cells. Expression of housekeeping genes such as beta-actin (mouse *Actb* and human *ACTB*) displayed relatively constant expression during the Affymetrix time-series (Fig. 1A,C). We examined the expression of other known cycling genes in the segmentation clock, including *HES5*, *HES7*, *HEY2*, *LFNG*, *AXIN2*, *NKD1*, and *SNAI1*. These genes were expressed at levels below the threshold of detection with the HG-U133 arrays or with only a fraction of time points crossing the threshold (*LFNG*, *SNAI1*). The cycling gene *HEY1* was identified independently as an oscillatory gene, described further below.

Next, we sought to identify additional gene candidates that displayed oscillatory expression in the human UCB1 microarray data set. We used Fourier analysis, an approach based on the fact that any time series can be expressed as a sum of sinusoids of different frequencies and amplitudes. It allows construction of a periodogram, a plot of the relative strength of each frequency component in the series. Significant oscillations at a particular frequency appear as peaks in this plot. We used the fast Fourier transform, an efficient algorithm that requires evenly spaced samples with no missing values, conditions we were able to meet due to the precise control of sample collection possible with cell culture. Then, we reduced this list from 4,491 gene probes to 1,409 candidates by eliminating probes that were absent in most samples and by visual inspection of time series (Fig. 2A, B; Supplemental Table S1). Of this list of 1,409 probes, 1,066 detected 953 annotated genes, including the known cycling genes *Hes1*, *Hey1*, and *Lfng*. The remaining 343 probes detected ESTs and other unannotated genes. We further supplemented this list with members of known segmentation clock pathways and homologues of somite development genes. We sampled 20 candidates for further analysis on the basis of several criteria, including robust oscillatory expression patterns, reports of expression in somites or presomitic mesoderm, and relatedness to known somitogenesis genes (Fig. 2C, D; Table 1). This list includes 3 genes in the notch signaling pathway (*MAML3*, *ID1*, *ID2*), 4 genes in the wnt pathway (*AXUD*, *CYR61*, *NKD2*, *TCF7L2*), a gene previously described as expressed in somites (*GLCCI1*; Ishikawa et al., 2004), and 12 other candidates, including the snail homologue *SNAI2* (Fig. 2C, D, Fig. 3 and Supplemental Fig. 2). The interpeak period for these genes was also consistent with 5 hours (Fig. 3).

In a cell culture model of the segmentation clock, genes that oscillate *in vitro* would also display oscillatory expression within the PSM. We examined mouse homologues for each of the 20

human oscillatory candidates using information from the NIH Unigene database (Table 1). We used mouse IMAGE cDNA clones to carry out whole mount *in situ* hybridization analysis of embryonic expression patterns (Figs. 4-6). We were able to clearly observe localized expression for nine genes. Of these nine, two were expressed strongly in the PSM (*Maml3* and *Nkd2*; Fig. 4,5) and two were expressed faintly in the PSM (*Glcci1*, *Tcf7l2*; Fig. 6). In addition, *Id1* and *Id2* were expressed in the somites but not clearly in the PSM using our assays (Fig. 6).

The expression patterns of *Maml3* and *Nkd2* were particularly intriguing. *Maml3* has not been characterized for expression in somite-stage embryos. In 8.5 dpc embryos, we observed expression in the neural tube and a broadly diffuse region of expression in the rostral PSM that varied in intensity relative to neural expression (Fig. 4A-C). This region was also observed in 9.0 dpc, 9.5 dpc, and 10.5 dpc embryos (Fig. 4D-H). Transverse sections confirmed localization of *Maml3* to the paraxial mesoderm and ventral neural tube within the rostral PSM (Fig. 4I). We next examined expression of *Maml3* relative to notch and wnt pathway cycling genes, *Mesp2*, and *Snai1*. We bisected fixed embryos, to determine relative position and expression levels. Comparison with *Mesp2*, which is expressed in the rostral −1 somite region, confirms that *Maml3* is expressed in a broad region centered on the −1 to −2 somite region, but extending further rostral and caudal as well (Fig. 4J, K). Representative comparisons of *Maml3* with *Lfng* (Fig. 4L), *Axin2* (Fig. 4M) and *Snai1* (Fig. 4N) indicate that *Maml3* is expressed in a broad rostral region that is dynamic in level but not in rostro-caudal extent in the PSM. By *in situ* hybridization alone, it was not possible to correlate expression levels of *Maml3* with phase of these cycling genes.

The wnt pathway gene *Nkd2* has been reported to be expressed in mouse PSM at 9.5 and 10.5 dpc (Wharton, 2001) but not described as an oscillatory gene. We observed expression of *Nkd2* by *in situ* hybridization in the caudal PSM and somites at 9.5 dpc (Fig. 5A, B) but not 8.5 dpc (data not shown). Higher levels of expression within somites was observed at 10.5 dpc (Fig. 5C) and the expression within the PSM was both variable in level and extent (Fig. 5D-F). Transverse sections confirmed expression of *Nkd2* in the paraxial mesoderm of the caudal PSM and in the tailbud mesoderm (Fig. 4G, H). Comparison with *Mesp2*, which is expressed in the rostral −1 somite region, confirms that *Nkd2* is expressed in a broad region at the caudal end of the PSM (Fig. 5I, J) similar to the caudal phases *Axin2* (Fig. 5L) and never extending to the rostral band of expression for *Lfng* (Fig. 5K) and *Snai1* (Fig. 5M). Based on *in situ* hybridization, it was not possible to correlate expression levels of *Nkd2* with phase of these cycling genes.

We also characterized expression of the seven other localized genes in 8.5 dpc, 9.5 dpc, and 10.5 dpc embryos. The wnt pathway gene *Tcf7l2* is faintly expressed in the rostral PSM in both 9.25 dpc and 8.5 dpc embryos (Fig. 6A,B). *Glcci1* (glucocorticoid induced transcript 1) is expressed in somites and in a faint band in the rostral PSM (Fig. 6C). We observed expression of the notch targets *Id1* and *Id2* in the somites, but not in the PSM (Fig. 6D,E). For *Ctgf* and *Nuak1*, we only observed gene expression in the developing neural tube and not in the paraxial mesoderm at these stages (Fig. 6F,G). *Slc2a3* was observed to be expressed in a punctate pattern on the surface ectoderm of the embryo and the dorsal neural tube (Fig. 6H). The additional 11 genes did not yield localized or detectable levels of expression by *in situ* hybridization.

Given the expression of *Maml3*, *Nkd2*, *Glcci1*, and *Tcf7l2*, we sought to examine if expression was dynamic in the PSM. To examine this, we bisected 9.5 dpc embryos in culture medium, collecting the left half immediately and allowing the right half to develop for an hour in culture conditions. We fixed split embryo halves for *in situ* hybridization analysis or collected them for RNA extraction for Q-PCR analysis. *In situ* hybridization analysis indicated that expression of *Maml3* and *Nkd2* varied in expression level over the 1 hour period (Fig. 7A,C), but did not

display the caudal to rostral shift in localized expression within the PSM, as observed in cycling genes such as *Lfng* (Fig. 7E). Quantitative PCR confirmed what was visually observed, with levels of *Nkd2* varying more than *Maml3*, but less than *Lfng* (Fig. 7B,D,F). Q-PCR data were normalized to the housekeeping gene *Gapdh*. To assay the periodicity of *Maml3* and *Nkd2* in mouse embryos, we also examined expression of these genes in split embryos cultured for 2 and 3 hours (Supplemental Fig. 3). We observed that levels of *Nkd2* returned to similar levels after 2-3 hours (Supplemental Fig. 3A,B) while *Maml3* expression differed at 1 and 2 hours, but returned to similar levels after 3 hours (Supplemental Fig. 3C,D). While consistent with an oscillatory period of approximately 2-3 hours in mouse embryos, the *in vitro* culturing conditions used for split embryos may lead to increased variability in periodicity. Given the low levels of PSM expression of *Glcci1* and *Tcf7l2*, we were unable to confirm variable expression in split embryos, either by *in situ* hybridization or by quantitative PCR.

We have examined expression of *Maml3* and *Nkd2* in two mutant lines that disrupt somitogenesis, *Dll3* and *Wnt3a*. In $Dll3^{pu/pu}$ embryos, *Lfng* cycling is disrupted but *Hes7* and *Hes1* display periodic expression (Kusumi et al. 2004). Unlike the $Dll1^{tm1Gos}$ mutation, which leads to loss of expression of many genes (Barrantes et al., 1999;Hrabé de Angelis et al., 1997;Jouve et al., 2000;Kokubo et al., 1999), the $Dll3^{pu}$ mutation is a more selective disruption of the segmentation clock. For *Maml3*, we observed that PSM expression is variable in 10.5 dpc $Dll3^{pu/pu}$ embryos, suggesting oscillatory expression (Fig. 8A-C; 10.5 dpc embryos were used to better visualize PSM expression of *Maml3*). However, the *Wnt3a* mutation completely disrupts expression of *Maml3* within the PSM (Fig. 8D-F). The $Wnt3a^{tm1Amc}$ mutation has previously been shown to disrupt expression of both *Axin2* and notch pathway members *Lfng* and *Hes1* (Aulehla et al., 2003). We observed that *Nkd2* expression is present in 9.5 dpc $Dll3^{pu/pu}$ embryos, with variable levels of *Nkd2* observed in mutants, suggesting potential oscillatory expression (Fig. 8G-I). In contrast, *Wnt3a* mutation completely disrupts expression of *Nkd2* within the PSM, but expression within the somites is still observed (Fig. 8J-L). These results are consistent with more severe disruptions in PSM and the segmentation clock due to the *Wnt3a* mutation.

Discussion

Using a mesenchymal stem cell model, we have demonstrated the first oscillatory expression of a segmentation clock gene (*HES1*) in human cells. This has allowed us to approximate a period for the human segmentation clock of 5 hours. Our analysis of a mouse C2C12 myoblast cell culture model confirmed a period of 2 hours, consistent with published *in vitro* analysis (Hirata et al., 2002) and embryonic studies (Barrantes et al., 1999). By using Affymetrix microarray based analysis, we have also been able to identify additional genes that display oscillatory expression *in vitro*, with top candidates examined by expression analysis of homologous genes in mouse embryos. This has identified oscillatory expression of the notch pathway gene *Maml3* and the wnt pathway gene *Nkd2* by whole mount and split embryo *in situ* hybridization analysis and confirmed by Q-PCR. Thus, we have shown that human and mouse *in vitro* models can recapitulate oscillatory expression observed *in embryo*. Additionally, we have identified over 1,400 gene probes that detect oscillatory expression in gene candidates and are available for further analysis (Supplemental Table S1).

Identification of segmentation clock genes with stationary oscillatory expression

Since the observation was reported of a notch pathway gene (*hairy*) that displayed dynamic cycling expression in the PSM of chick embryos (Palmeirim et al., 1997), the number of genes and pathways displaying oscillatory expression during somitogenesis in the mouse, chick, and zebrafish models, as identified by *in situ* hybridization, has steadily grown to include *Lfng, Hes1, Hes7, Hey1, Hey2, Axin2, Nkd1,* and *Snai1* (Aulehla & Johnson, 1999; Bessho et al.,

2001a; Bessho et al., 2001b; Barrantes et al., 1999;Dale et al., 2006;Dunwoodie et al., 2002;Forsberg et al., 1998;Jiang et al., 2000;Jouve et al., 2000;Leimeister et al., 1999;Leimeister et al., 2000a;McGrew et al., 1998;Nakagawa et al., 1999). The technique of *in situ* hybridization is semi-quantitative, so genes with cycling changes in expression pattern (oscillatory changes in pattern from the caudal to rostral PSM) are more readily detected than genes that oscillate in expression level but not in spatial localization. Microarray and Q-PCR methods are quantitative, so it is possible to detect oscillatory changes in expression level in cell culture models and in embryonic tissues.

Quantitative analysis of our 20 candidate genes has identified two genes, *Maml3* and *Nkd2*, which display oscillatory changes in level but not in spatial localization within the PSM. This pattern differs from “cycling” genes, such as *Lfng*, which display caudal-to-rostral shifts in expression pattern and quantitative changes in expression level (Fig. 9A). *Maml3* and *Nkd2* expression also differs from “stage-specific” genes such as *Mesp2*, which is expressed in a stripe within the PSM that varies in length during the somite cycle (Fig. 9A). Thus, *Maml3* and *Nkd2* display stationary oscillatory expression within the PSM, i.e., gene expression levels are dynamic but the boundaries of gene expression patterns may display subtle variations but are relatively constant (Fig. 9B). Genes which are stationary by spatial localization but display oscillatory expression levels may play a role in the activation or repression of genes specifically in those regions, e.g. the caudal PSM or the rostral PSM. These stationary oscillatory genes could interact with cycling components of the segmentation clock, or they could be involved in refining the output of the segmentation clock. Clearly, the PSM can be divided into regions based on boundary formation, rostral-caudal boundary patterning, and segmental determination (reviewed in Dubrulle & Pourquié, 2004b) or for expression of regulators *Fgf8* (Dubrulle & Pourquié, 2004a) and *Raldh* (Vermot et al., 2005). Even genes with cycling expression, such as *Lfng* and *Nkd1*, display expression in the caudal-most PSM that varies in expression level but does not exhibit the anterograde spatial shifts in pattern (Forsberg et al., 1998;Ishikawa et al., 2004;Kusumi et al., 2004). Stationary oscillatory genes may serve to mark subdomains within the PSM with differential activation or repression of notch, wnt, or other signaling pathways. Given that the quantitative changes of stationary oscillatory genes may be difficult to identify by semi-quantitative methods such as *in situ* hybridization, it is possible that additional genes of this type may have been overlooked. Further analysis of these oscillatory candidate genes may help to determine their roles relative to cycling components of the segmentation clock.

Given the large number of candidate genes identified in our screen, there may be additional genes with this expression profile within the PSM. Functional genomic approaches have been used by other groups to identify genes expressed within paraxial mesodermal tissue (Buttitta et al., 2003;Ishikawa et al., 2004;Tonegawa et al., 2003) or disrupted in notch pathway mutations (Machka et al., 2005 for $Dll1^{tm1Gos}$). Genes identified in these screens were compared with genes selected from our Fourier analysis and used to identify top candidates (Table 1). For example, *Glcci1* and *Nkd2* were previously identified as being expressed in PSM and somite, but not as displaying dynamic expression (Ishikawa et al., 2004;Wharton et al., 2001). A recent microarray study of mouse PSM tissues used *in situ* hybridization to determine the phase of PSM tissue within the somite cycle and to construct an extrapolated segmentation clock period (Dequeant et al., 2006). This approach is different from our synchronized mesenchymal stem cell-based study. First, we have observed periodic oscillations of *HES1* in real time over 24 hours, as opposed to the estimated single cycle based on *in situ* hybridization analysis of split embryo PSM halves. Second, we have examined cells at the onset of synchronized oscillation, while Dequeant et al. have assayed mouse embryos in mid-somitogenesis. There is a subset of oscillatory candidates in common between our data set and that of Dequeant et. al., including the known cycling genes *Hes1* and *Hey1* and the newly identified oscillatory genes *Id1* and *Klf10*. Interestingly, *Nkd2* was not identified in the screen

of Dequeant et al., and the Affymetrix MOE430A array used by these investigators does not contain probes to detect *Maml3*. Conversely we did not identify genes such as *BCL2L11, EFNA1, MYC, NRARP,* and *SP5* due to low expression levels in UCB1 cells, or *DKK1, DUSP6, HAS2, PHLDA1,* and *SPRY2* due to absence of periodic expression in UCB1. Comparison of our 1,409 human gene probe candidates (detecting 953 annotated genes) with the 3,000 oscillatory mouse gene probes from Dequeant et al. reveals 119 genes in common, including genes in the notch pathway (*HES1, HEY1, ID1, ID2, TLE3*), the wnt pathway (*AXIN1, AXUD, CYR61, DACT1, DKK1, PHLDA1*) and the Fgf pathway (*FGF2, FGFR1OP2*; Supplemental Table S1). Further characterization of these 119 genes could identify additional oscillatory gene components of the segmentation clock.

The segmentation clock modeled in human mesenchymal stem cells

Given the inability to examine early events in human development, no information has been available about oscillatory genes or clock-rate in the human segmentation clock. We have used functional genomic techniques to examine synchronized human UCB1 mesenchymal stem cells. These UCB1 cells have been extensively characterized by Affymetrix microarrays for expression profile and display differentiation capacity similar to the multipotent cells in the PSM (Markov et al., in press). Intriguingly, the oscillations of *HES1* in the human cells displayed an approximately 5 hour periodicity over 24 hours, which would be the equivalent of 4 to 5 cycles per day. Embryological studies of human embryos from the 1940s have suggested a rate of approximately 3-4 somites per day (Sadler, 2000), which is roughly consistent with our findings. The rate of mouse somitogenesis also varies during embryogenesis, ranging from 1.5-2 hours in the trunk somites to 2-3 hours in the tail somites (Gossler & Tam, 2002). At 5 hours, the human clock-rate would be over twice as long as that of the mouse, and one would expect that autoregulatory factors such as *HES1* and *HES7* might display significantly altered mRNA and protein stabilities. Analysis of the half-life of mRNA and protein for genes such as *Hes7* have identified that stability of the segmentation clock components is tightly correlated with the species-specific clock rate (Hirata et al., 2004).

The slower dynamics of the human segmentation clock will need to be considered in the etiology of vertebral birth defects. In the mouse, *Dll1*, *Dll3*, *Hes7*, *Lfng*, *Notch1* and *Psen1* mutants display segmental patterning defects (Barrantes et al., 1999;Bessho et al, 2001;Conlon et al., 1995;Dunwoodie et al., 2002;Evrard et al., 1998;Hrabé de Angelis et al., 1997; Kusumi et al., 1998; Zhang & Gridley, 1998). Mutations in the human segmentation clock genes *DLL3, MESP2,* and *LFNG* have been identified in rare, recessive forms of several vertebral defect syndromes, but the majority of spinal defects are less severe and appear to have multifactorial etiology (Bulman et al., 2000;Whittock et al., 2003;Sparrow et al., 2006; Maisenbacher et al., 2006). Clearly, environmental insults isolated to a limited time period could affect the formation of fewer segments in humans than in mice, but even disruption of a single human vertebra such as a wedge or hemi-vertebra can lead to severe spinal curves (Erol et al., 2004). While somitogenesis in the mouse is completed within 4-5 days, segmentation in humans can take place over a period almost 3 times as long, presenting a longer time window of susceptibility for environmental perturbations.

Availability of a cell culture model of the human segmentation clock now permits us to specifically activate or repress known mediators of oscillatory signaling using gene constructs and environmental agents. For example, notch pathway signaling could be inhibited using gamma-secretase inhibitors such as DAPT, and Notch receptor activation could be induced by calcium chelators such as EGTA/EDTA. A cell culture model also allows for testing of environmental and genetic factors that may affect susceptibility to segmental malformations seen in spinal birth defects. Interestingly, glucocorticoid induced transcript 1 (*Glcci1*), one of the genes that we identified as expressed in the somites and PSM (Fig. 6C), was also found in

a microarray-based screen of genes expressed in somites (Ishikawa et al., 2004). There is a surge of corticosterone production late in fetal life, and glucocorticoids play a role in development of many organs and tissues (Cole et al., 1995). A role in somitogenesis has not been explored. Oscillatory expression of *GLCCI1*, which is induced in response to glucocorticoid induction, may be relevant in pursuing the effects of intra-uterine factors on somitogenesis and the etiology of birth defects. The effects of environmental factors can be examined using the UCB1 mesenchymal stem cell model, and effects on notch and wnt pathway oscillations can be monitored.

Compilation and comparison of data from this and other functional genomic studies of the segmentation clock will be useful for several efforts. Bioinformatic analysis of genomic sequence around oscillatory genes may help to identify common transcriptional binding sites. Additional functional genomic analysis of the segmentation clock in organisms with shorter periodicities, such as zebrafish (30 min.) and chick (90 min.) will also help in identifying commonality and divergences in the oscillatory genes among vertebrates. The growing list of somite clock genes and their immediate downstream targets will help to build the candidate gene list for ongoing clinical genetic studies of segmentation defects.

Supplementary Material

Refer to Web version on PubMed Central for supplementary material.

Acknowledgements

We thank Mizuho Mimoto, Michael Barton, Megan O'Brien, Neha Sahni, Michelle Segalov, and Stacey Stevens for technical assistance, and Terry Yamaguchi and Alan Rawls for their kind gift of the *Wnt3a*^{tm1Amc} mouse line. We thank Saeed Tavazoie for helpful discussions and Jeanne Wilson-Rawls for commenting on our manuscript. KK is a recipient of a Burroughs Wellcome Fund Hitchings-Elion Fellowship, and this work was funded by NIH RO1 AR050687 to KK.

References

Aulehla A, Herrmann BG. Segmentation in vertebrates: clock and gradient finally joined. Genes Dev 2004;18:2060–7. [PubMed: 15342488]

Aulehla A, Johnson RL. Dynamic expression of lunatic fringe suggests a link between notch signaling and an autonomous cellular oscillator driving somite segmentation. Dev Biol 1999;207:49–61. [PubMed: 10049564]

Aulehla A, et al. Wnt3a plays a major role in the segmentation clock controlling somitogenesis. Dev Cell 2003;4:395–406. [PubMed: 12636920]

Baksh D, et al. Adult mesenchymal stem cells: characterization, differentiation, and application in cell and gene therapy. J Cell Mol Med 2004;8:301–16. [PubMed: 15491506]

Barrantes, I. d. B., et al. Interaction between *Notch* signalling and *Lunatic fringe* during somite boundary formation in the mouse. Curr. Biol 1999;9:470–480. [PubMed: 10330372]

Bessho Y, et al. Periodic repression by the bHLH factor Hes7 is an essential mechanism for the somite segmentation clock. Genes Dev 2003;17:1451–6. [PubMed: 12783854]

Bessho Y, et al. Hes7: a bHLH-type repressor gene regulated by Notch and expressed in the presomitic mesoderm. Genes Cells 2001;6:175–85. [PubMed: 11260262]

Bessho Y, et al. Dynamic expression and essential functions of Hes7 in somite segmentation. Genes Dev 2001;15:2642–7. [PubMed: 11641270]

Bulman MP, et al. Mutations in the human delta homologue, DLL3, cause axial skeletal defects in spondylocostal dysostosis. Nat Genet 2000;24:438–41. [PubMed: 10742114]

Buttitta L, et al. Microarray analysis of somitogenesis reveals novel targets of different WNT signaling pathways in the somitic mesoderm. Dev Biol 2003;258:91–104. [PubMed: 12781685]

Caplan AI. The mesengenic process. Clin Plast Surg 1994;21:429–35. [PubMed: 7924141]

Cole TJ, et al. Targeted disruption of the glucocorticoid receptor gene blocks adrenergic chromaffin cell development and severely retards lung maturation. Genes Dev 1995;9:1608–21. [PubMed: 7628695]

Conlon RA, et al. Notch1 is required for the coordinate segmentation of somites. Development 1995;121:1533–45. [PubMed: 7789282]

Dale JK, et al. Oscillations of the snail genes in the presomitic mesoderm coordinate segmental patterning and morphogenesis in vertebrate somitogenesis. Dev Cell 2006;10:355–66. [PubMed: 16516838]

Deans RJ, Moseley AB. Mesenchymal stem cells: biology and potential clinical uses. Exp Hematol 2000;28:875–84. [PubMed: 10989188]

Dequeant ML, et al. A Complex Oscillating Network of Signaling Genes Underlies the Mouse Segmentation Clock. 200610.1126/science.1133141

Dubrulle J, Pourquie O. fgf8 mRNA decay establishes a gradient that couples axial elongation to patterning in the vertebrate embryo. Nature 2004;427:419–22. [PubMed: 14749824]

Dubrulle J, Pourquie O. Coupling segmentation to axis formation. Development 2004;131:5783–93. [PubMed: 15539483]

Dunwoodie SL, et al. Axial skeletal defects caused by mutation in the spondylocostal dysplasia/pudgy gene Dll3 are associated with disruption of the segmentation clock within the presomitic mesoderm. Development 2002;129:1795–806. [PubMed: 11923214]

Erol B, et al. Congenital scoliosis and vertebral malformations: characterization of segmental defects for genetic analysis. J Pediatr Orthop 2004;24:674–82. [PubMed: 15502569]

Evrard YA, et al. lunatic fringe is an essential mediator of somite segmentation and patterning. Nature 1998;394:377–81. [PubMed: 9690473]

Forsberg H, et al. Waves of mouse Lunatic fringe expression, in four-hour cycles at two-hour intervals, precede somite boundary formation. Curr Biol 1998;8:1027–30. [PubMed: 9740806]

Giudicelli F, Lewis J. The vertebrate segmentation clock. Curr Opin Genet Dev 2004;14:407–14. [PubMed: 15261657]

Gossler, A.; Tam, PPL. Mouse development. Academic Press; San Diego, CA: 2002. Somitogenesis: Segmentation of the paraxial mesoderm and the delineation of tissue compartments; p. 127-149.

Hirata H, et al. Instability of Hes7 protein is crucial for the somite segmentation clock. Nat Genet 2004;36:750–4. [PubMed: 15170214]

Hirata H, et al. Oscillatory expression of the bHLH factor Hes1 regulated by a negative feedback loop. Science 2002;298:840–3. [PubMed: 12399594]

Hirsinger E, et al. Somite formation and patterning. Int Rev Cytol 2000;198:1–65. [PubMed: 10804460]

Hrabe de Angelis M, et al. Maintenance of somite borders in mice requires the Delta homologue DII1. Nature 1997;386:717–21. [PubMed: 9109488]

Ishikawa A, et al. Mouse Nkd1, a Wnt antagonist, exhibits oscillatory gene expression in the PSM under the control of Notch signaling. Mech Dev 2004;121:1443–53. [PubMed: 15511637]

Iulianella A, et al. Somitogenesis: breaking new boundaries. Neuron 2003;40:11–4. [PubMed: 14527429]

Javazon EH, et al. Mesenchymal stem cells: paradoxes of passaging. Exp Hematol 2004;32:414–25. [PubMed: 15145209]

Jiang YJ, et al. Notch signalling and the synchronization of the somite segmentation clock. Nature 2000;408:475–9. [PubMed: 11100729]

Jouve C, et al. Notch signalling is required for cyclic expression of the hairy-like gene HES1 in the presomitic mesoderm. Development 2000;127:1421–9. [PubMed: 10704388]

Keynes RJ, Stern CD. Segmentation in the vertebrate nervous system. Nature 1984;310:786–9. [PubMed: 6472458]

Keynes RJ, Stern CD. Mechanisms of vertebrate segmentation. Development 1988;103:413–29. [PubMed: 3073078]

Kokubo H, et al. Identification and expression of a novel family of bHLH cDNAs related to Drosophila hairy and enhancer of split. Biochem Biophys Res Commun 1999;260:459–65. [PubMed: 10403790]

Kusumi K, et al. Dll3 pudgy mutation differentially disrupts dynamic expression of somite genes. Genesis 2004;39:115–21. [PubMed: 15170697]

Leimeister C, et al. Oscillating expression of c-Hey2 in the presomitic mesoderm suggests that the segmentation clock may use combinatorial signaling through multiple interacting bHLH factors. Dev Biol 2000a;227:91–103. [PubMed: 11076679]

Leimeister C, et al. Hey genes: a novel subfamily of hairy- and Enhancer of split related genes specifically expressed during mouse embryogenesis. Mech Dev 1999;85:173–7. [PubMed: 10415358]

Leimeister C, et al. Analysis of HeyL expression in wild-type and Notch pathway mutant mouse embryos. Mech Dev 2000b;98:175–8. [PubMed: 11044625]

Machka C, et al. Identification of Dll1 (Delta1) target genes during mouse embryogenesis using differential expression profiling. Gene Expr Patterns 2005;6:94–101. [PubMed: 15979417]

Maisenbacher MK, et al. Molecular analysis of congenital scoliosis: a candidate gene approach. Hum Genet 2005;116:416–9. [PubMed: 15717203]

Markov V, et al. Identification of distinct cord blood-derived mesenchymal stem/stromal cells with different growth kinetics, differentiation potentials, and gene expression profiles. Stem Cells Dev 2007;16:1–21. [PubMed: 17348800]

Masamizu Y, et al. Real-time imaging of the somite segmentation clock: revelation of unstable oscillators in the individual presomitic mesoderm cells. Proc Natl Acad Sci U S A 2006;103:1313–8. [PubMed: 16432209]

McGrew MJ, et al. The lunatic fringe gene is a target of the molecular clock linked to somite segmentation in avian embryos. Curr Biol 1998;8:979–82. [PubMed: 9742402]

McGrew MJ, Pourquie O. Somitogenesis: segmenting a vertebrate. Curr Opin Genet Dev 1998;8:487–93. [PubMed: 9729727]

Murray SA, Gridley T. Snail1 Gene Function During Early Embryo Patterning in Mice. Cell Cycle 2006;5

Nakagawa O, et al. HRT1, HRT2, and HRT3: a new subclass of bHLH transcription factors marking specific cardiac, somitic, and pharyngeal arch segments. Dev Biol 1999;216:72–84. [PubMed: 10588864]

Palmeirim I, et al. Avian hairy gene expression identifies a molecular clock linked to vertebrate segmentation and somitogenesis. Cell 1997;91:639–48. [PubMed: 9393857]

Pourquie O. Vertebrate somitogenesis: a novel paradigm for animal segmentation? Int J Dev Biol 2003;47:597–603. [PubMed: 14756335]

Roufosse CA, et al. Circulating mesenchymal stem cells. Int J Biochem Cell Biol 2004;36:585–97. [PubMed: 15010325]

Sadler, TW. Langman's Medical Embryology. Williams & Wilkins; Baltimore, MD: 2000.

Saga Y, et al. Mesp2: a novel mouse gene expressed in the presegmented mesoderm and essential for segmentation initiation. Genes Dev 1997;11:1827–39. [PubMed: 9242490]

Saga Y, Takeda H. The making of the somite: molecular events in vertebrate segmentation. Nat Rev Genet 2001;2:835–45. [PubMed: 11715039]

Sato Y, et al. Morphological boundary forms by a novel inductive event mediated by Lunatic fringe and Notch during somitic segmentation. Development 2002;129:3633–44. [PubMed: 12117813]

Sparrow DB, et al. Mutation of the LUNATIC FRINGE gene in humans causes spondylocostal dysostosis with a severe vertebral phenotype. Am J Hum Genet 2006;78:28–37. [PubMed: 16385447]

Takahashi Y, et al. *Mesp2* initiates somite segmentation through the *Notch* signalling pathway. Nat Genet 2000;25:390–6. [PubMed: 10932180]

Tam PP. The control of somitogenesis in mouse embryos. J Embryol Exp Morphol 1981;65(Suppl):103–28. [PubMed: 6801176]

Tam PP, Trainor PA. Specification and segmentation of the paraxial mesoderm. Anat Embryol (Berl) 1994;189:275–305. [PubMed: 8074321]

Tonegawa A, et al. Systematic screening for signaling molecules expressed during somitogenesis by the signal sequence trap method. Dev Biol 2003;262:32–50. [PubMed: 14512016]

Vermot J, Pourquie O. Retinoic acid coordinates somitogenesis and left-right patterning in vertebrate embryos. Nature 2005;435:215–20. [PubMed: 15889094]

Wharton KA Jr. et al. Vertebrate proteins related to Drosophila Naked Cuticle bind Dishevelled and antagonize Wnt signaling. Dev Biol 2001;234:93–106. [PubMed: 11356022]

Whittock NV, et al. Molecular genetic prenatal diagnosis for a case of autosomal recessive spondylocostal dysostosis. Prenat Diagn 2003;23:575–9. [PubMed: 12868087]

Wilkinson, DG. In situ hybridisation, a practical approach. Oxford University Press; Oxford: 1992. Whole mount in situ hybridisation of vertebrate embryos; p. 75-83.

Zhang N, Gridley T. Defects in somite formation in lunatic fringe-deficient mice. Nature 1998;394:374–7. [PubMed: 9690472]

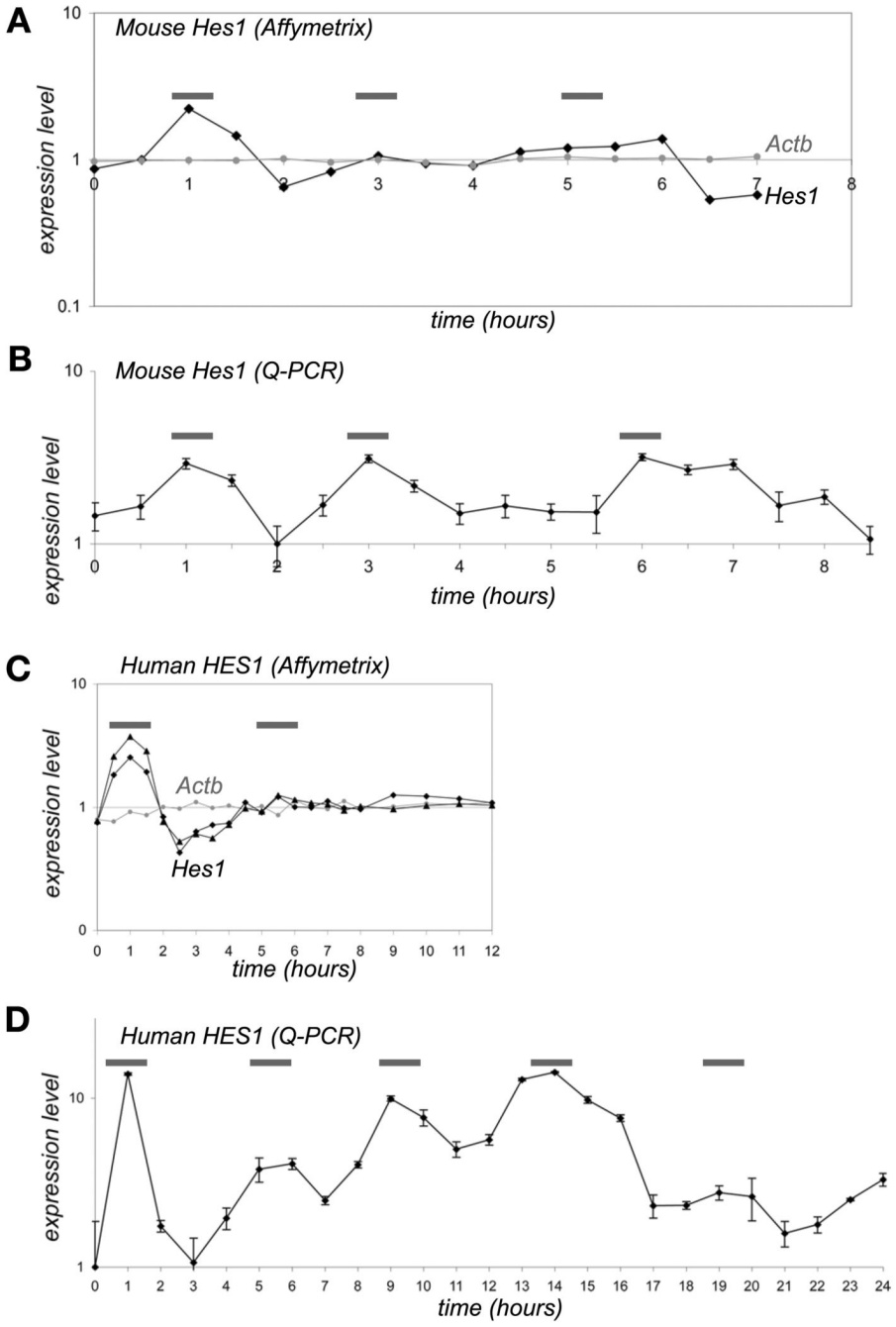

Figure 1.

Oscillatory expression of the notch pathway gene *Hes1* in synchronized mouse C2C12 myoblasts (A,B) and *HES1* in synchronized human mesenchymal stem cells (C,D). Cells were synchronized by treatment in low-serum conditions, and restoration of normal serum levels induced oscillation of notch pathway genes. Robust multichip averaging methods were used to normalize microarray data, and levels of housekeeping genes such as beta-actin were relatively constant (gray lines in A, MOE430v2; C, HG-U133A). Affymetrix MOE430Av2 (A) and quantitative PCR (B) results for *Hes1* expression in mouse C2C12 myoblasts are shown, with an oscillation period of 2 hours, consistent with previously published reports for mouse cells in cell culture (Hirata et al., 2002) and correlating with the average periodicity in

mouse embryos (Gossler & Tam, 2002). Affymetrix HG-U133A (C) and quantitative PCR (D) results for *HES1* expression in human UCB1 cells are shown with an oscillation period of approximately 5 hours. Quantitative PCR data points are shown with error bars indicating one SD. Gray bars indicate oscillatory peak regions (A-D).

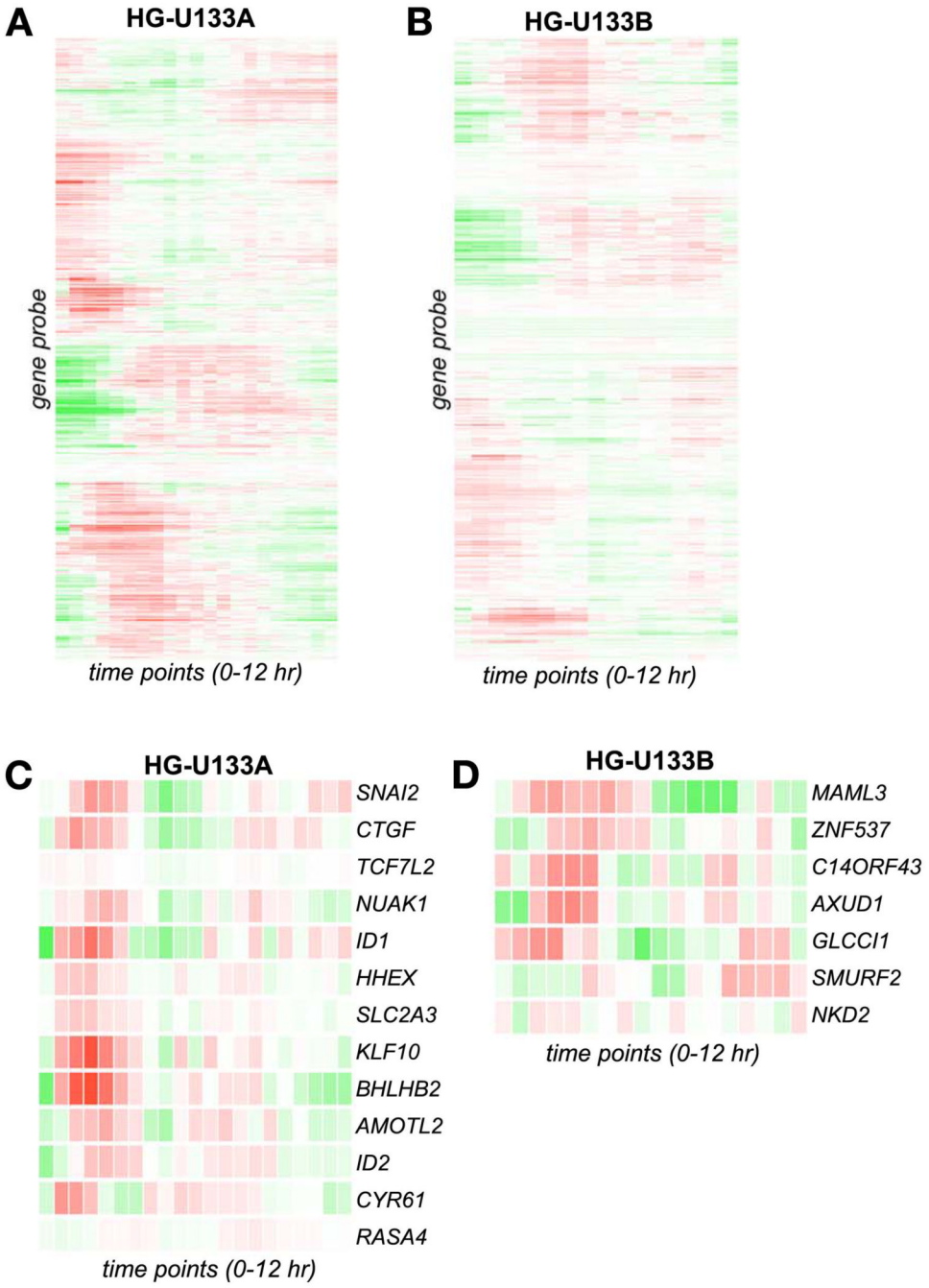

Figure 2.

Diagrams illustrating the levels of candidate oscillatory expression genes, assayed by Affymetrix microarray. Red indicates increased expression and green decreased expression relative to the mean level in the displayed HEAT map. Candidates were identified by Fourier analysis of expression time series (A, 824 gene probes on the HG-U133A array and B, 585 gene probes on the HG-U133B array). Additional analysis was used to identify the top 20 gene candidates, illustrated on C (HG-U133A array) and D (HG-U133B array).

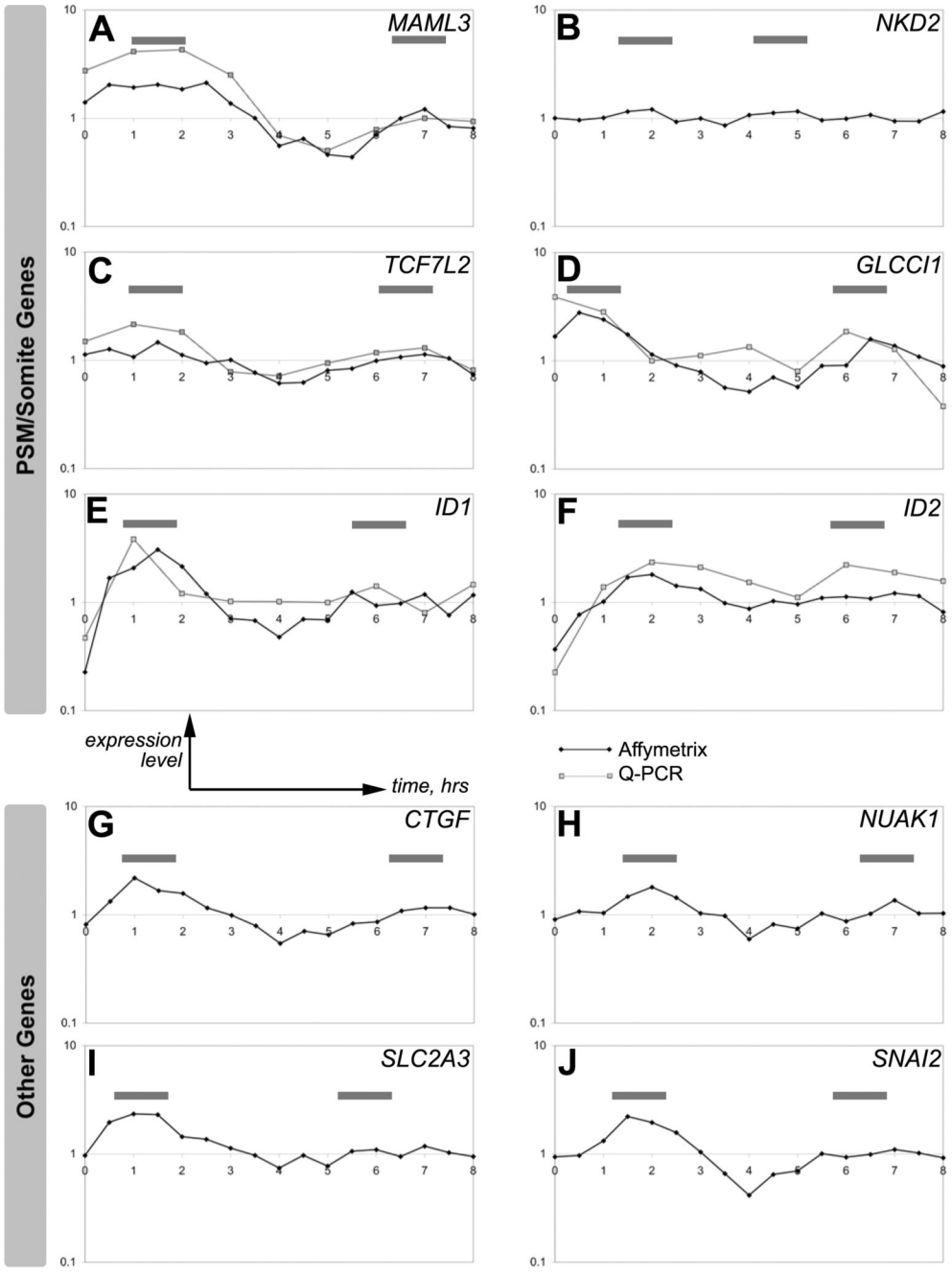

Figure 3.

Identification of genes with oscillatory expression in synchronized mesenchymal stem cells by Affymetrix HG-U133 microarray analysis. Genes with oscillatory expression were identified by Fourier analysis and cluster analysis, and the mouse homologues of 20 top candidate genes were selected for embryonic analysis. Shown are the gene expression levels of 9 genes that displayed localized expression in 9.5 dpc embryos: the notch pathway gene *MAML3* (A), the wnt pathway genes *NKD2* (B) and *TCF7L2* (C), the glucocorticoid induced gene *GLCCI1* (D), the notch target genes *ID1* (E) and *ID2* (F), and the genes *CTGF* (G), *NUAK1* (H), and *SLC2A3* (I). In addition, the expression time series for the snail homologue *SNAI2* (J) is shown. Expression data for 8 hours is shown with microarray results (black line)

and quantitative PCR results (gray line). Expression values are shown on a logarithmic scale. Levels of *NKD2* were below the threshold of detection by Q-PCR. Gray bars indicate oscillatory peak regions (A-J).

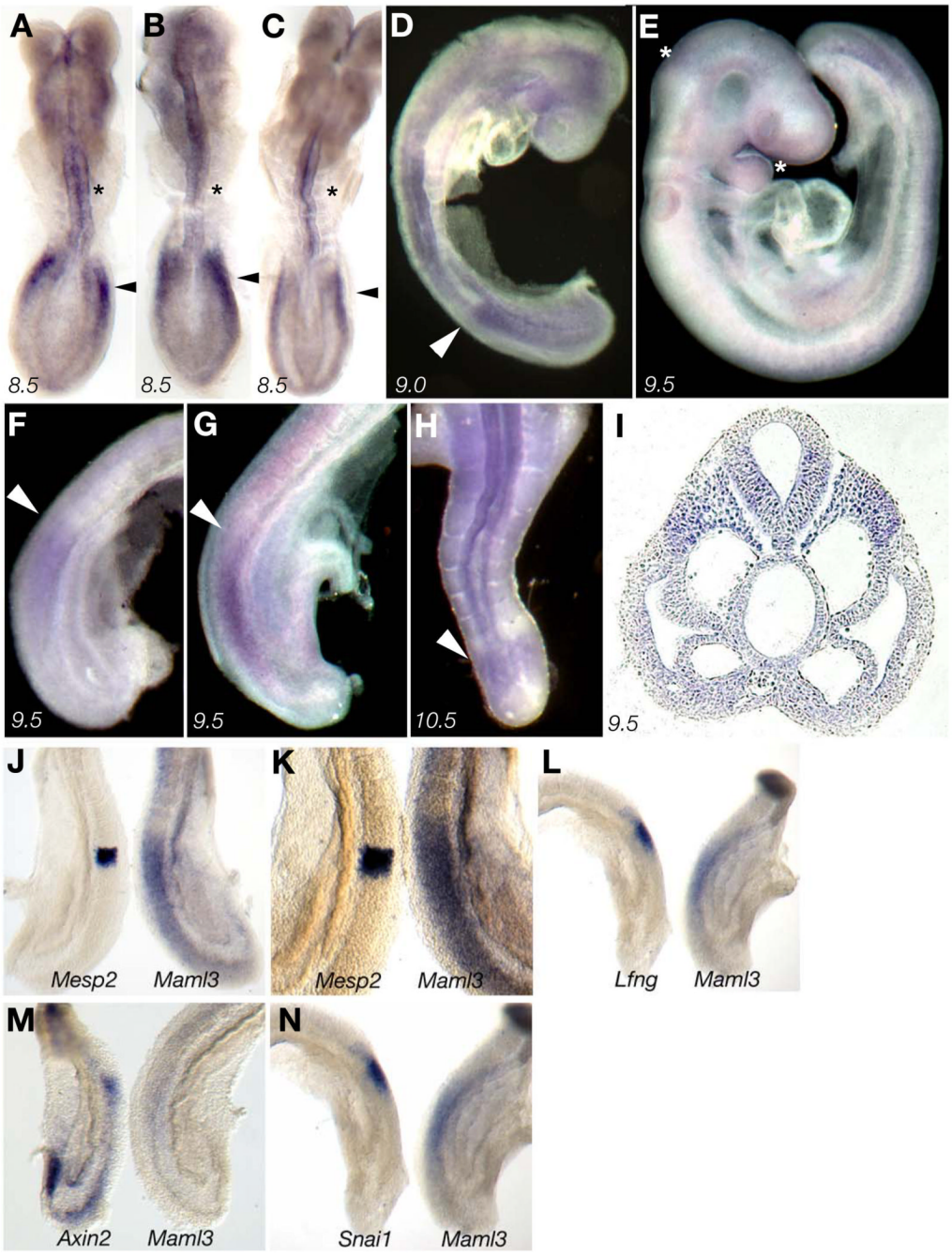

Figure 4.

Localized expression of the notch pathway gene *Maml3* in 8.5 dpc (A-C), 9.0 dpc (D), 9.5 dpc (E-G) and 10.5 dpc (H) mouse embryos, as determined by whole mount *in situ* hybridization. *Maml3* expression in the rostral presomitic mesoderm is detectable beginning at 8.5 dpc stage (A-C), with levels of expression within the PSM varying (arrowheads) relative to expression in the neural tube (asterisks). Expression in 9.5 dpc embryos was also present in the first pharyngeal arch and caudal midbrain (asterisks in E). Localization of expression of *Maml3* within the PSM is similar in 10.5 dpc embryos (H). Transverse section from the rostral PSM demonstrates that *Maml3* is expressed in the paraxial mesoderm and ventral neural of a 9.5 dpc embryo (I). Localized expression of *Maml3*, compared to the rostral PSM marker *Mesp2* (J

and magnified in K) and known cycling genes in the notch pathway (*Lfng*; L), wnt pathway (*Axin2*; M), snail (*Snai1*; N), in microdissected PSM halves. Expression of 9.5 dpc embryos was analyzed by whole mount *in situ* hybridization of microdissected PSM halves, with gene expression patterns compared. The broad region of *Maml3* expression extends further rostrally than *Mesp2* (J,K; n=4) and uniquely marks a region within the presomitic mesoderm extending from the rostral bands of expression of *Lfng* (L; n=5), *Axin2* (M; n=4), and *Snai1* (N; n=3) but diminishing prior to the tailbud region.

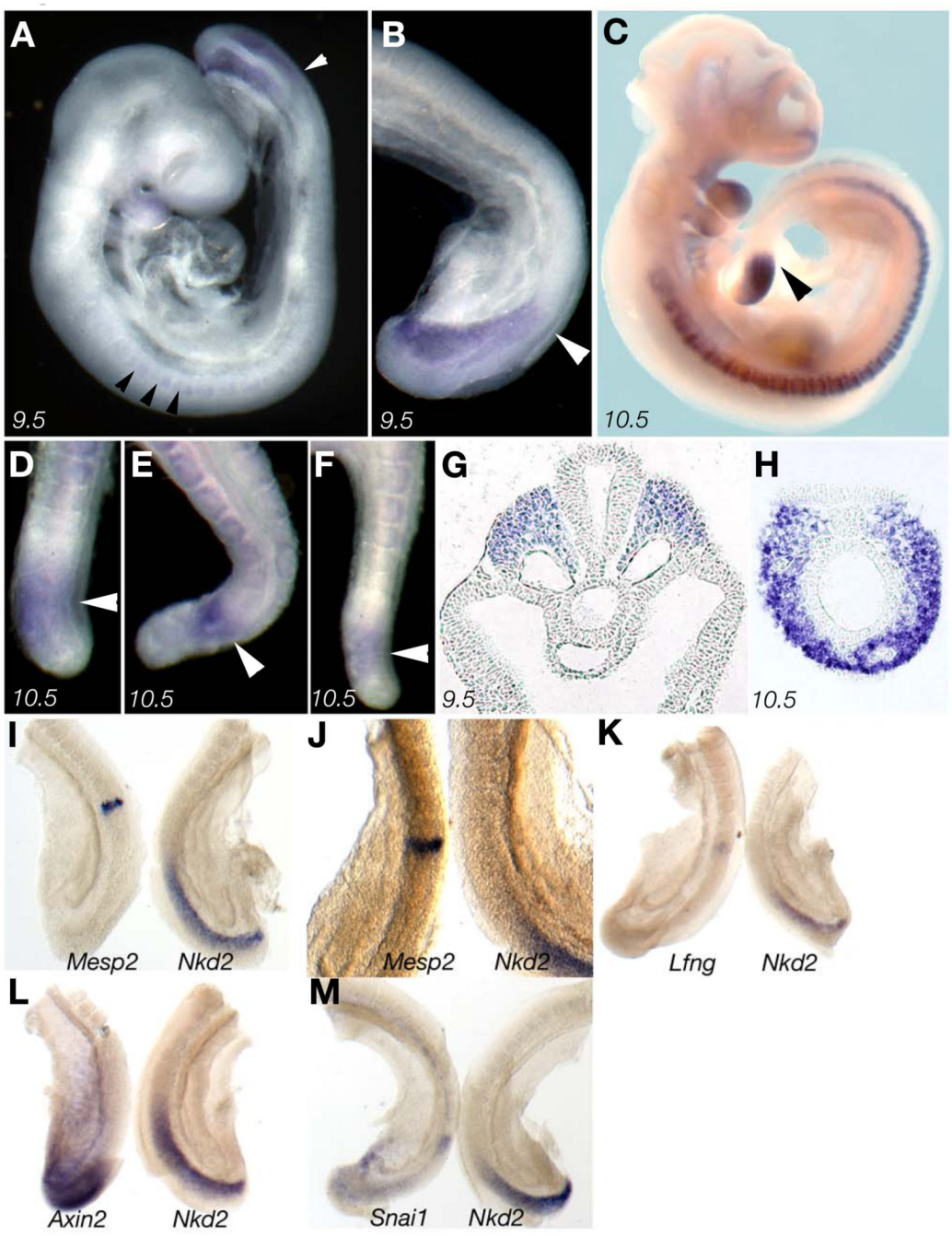

Figure 5.

Localized expression of the wnt pathway gene *Nkd2* in 9.5 dpc (A, B) and 10.5 dpc (C-F) mouse embryos determined by whole mount *in situ* hybridization. *Nkd2* expression in the caudal presomitic mesoderm is detectable beginning at 9.5 dpc stage (A, B; white arrowheads), with no expression visible at 8.5 dpc (data not shown). Low levels of expression are also present in maturing somites (A; black arrowheads) and in the rostral region of the first pharyngeal arch. Localization of expression of *Nkd2* is similar in 10.5 dpc (C; black arrowhead), with higher levels of expression observed in the somites (C). Levels of *Nkd2* expression within the PSM were variable (arrowheads), as shown in three PSM regions from 10.5 dpc embryos (D-F). Transverse sections from the caudal PSM of a 9.5 dpc embryo clearly show *Nkd2* expression

localized to the paraxial mesoderm (G) and in the tailbud mesoderm of a 10.5 dpc embryo (H, dorsal is at top). Localized expression of *Nkd2*, compared to the rostral PSM marker *Mesp2* (I and magnified in J) and known cycling genes in the notch pathway (*Lfng*; K), wnt pathway *(Axin2*; L), snail (*Snai1*; M) in 9.5 dpc microdissected PSM halves. Expression in 9.5 dpc embryos was analyzed by whole mount *in situ* hybridization of microdissected PSM halves. For *Nkd2*, the broad region of PSM expression is caudal to the rostral PSM band of *Lfng* (K; n=8) and *Mesp2* (I, J; n=4) and is expressed over a broader region than the caudal zone of expression of *Axin2* (L; n=8) and *Snai1* (M; n=4).

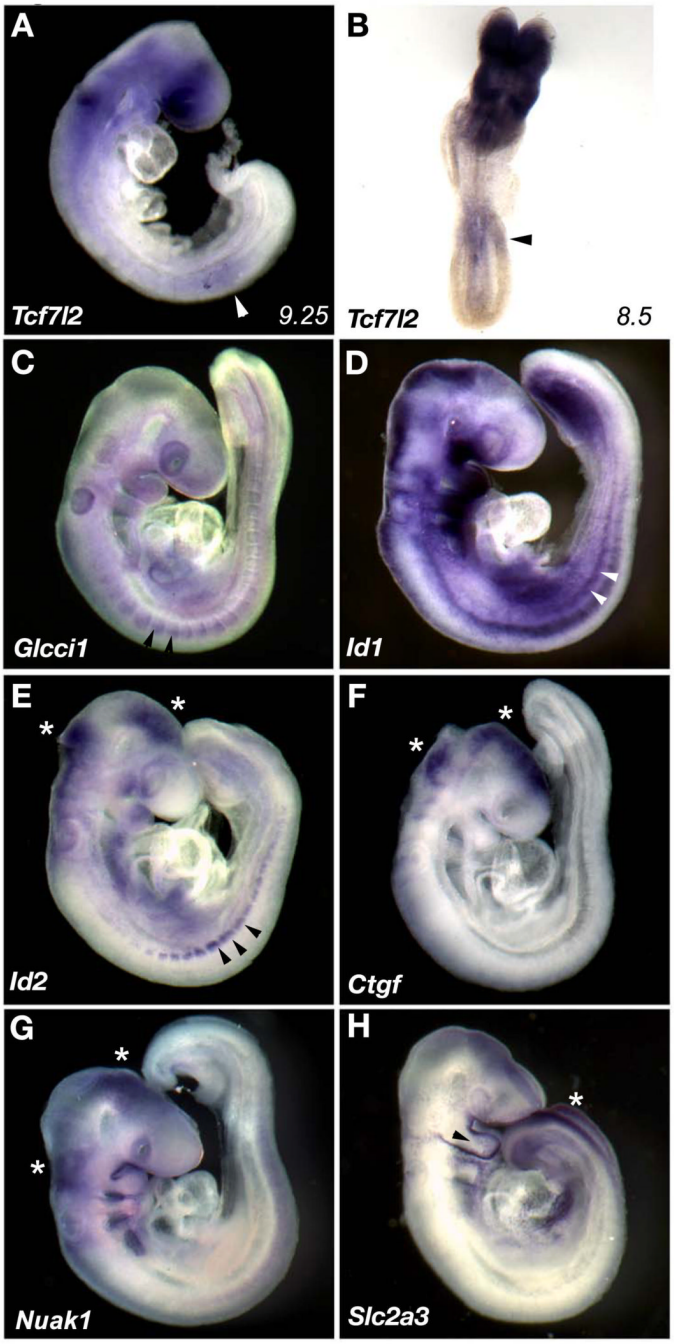

Figure 6.

Expression of additional oscillatory gene candidates in 9.5 dpc mouse embryos. Mouse genes homologous to oscillatory genes identified in the human MSC microarray screen were determined as described. Whole mount *in situ* hybridization was used to determine expression patterns of 20 candidate genes. Selected genes with localized expression in 9.5 dpc embryos, including the wnt pathway gene *Tcf7l2* (A,B), the glucocorticoid induced transcript 1 (*Glcci1;* C), the notch pathway genes *Id1* and *Id2* (D,E), connective tissue growth factor (*Ctgf*; F), the protein kinase *Nuak*1 (G), and *Slc2a3* (H), are shown. We observed genes with expression in the paraxial mesoderm. Specifically, low levels of expression in the presomitic mesoderm are observed in *Tcf7l2* (A, 9.5 dpc; B, 8.5 dpc; indicated with arrowheads) and

Glcci1 (C). Somitic expression is observed in *Glcci1* (C), *Id1* (D), and *Id2* (E), marked with arrowheads. Expression in the developing neural tube and/or pharyngeal arches (indicated by asterisks) is also observed for Id2 (E), Ctgf (F), Nuak1 (G), and *Slc2a3* (H). *Slc2a3* is also expressed in the surface ectoderm (H).

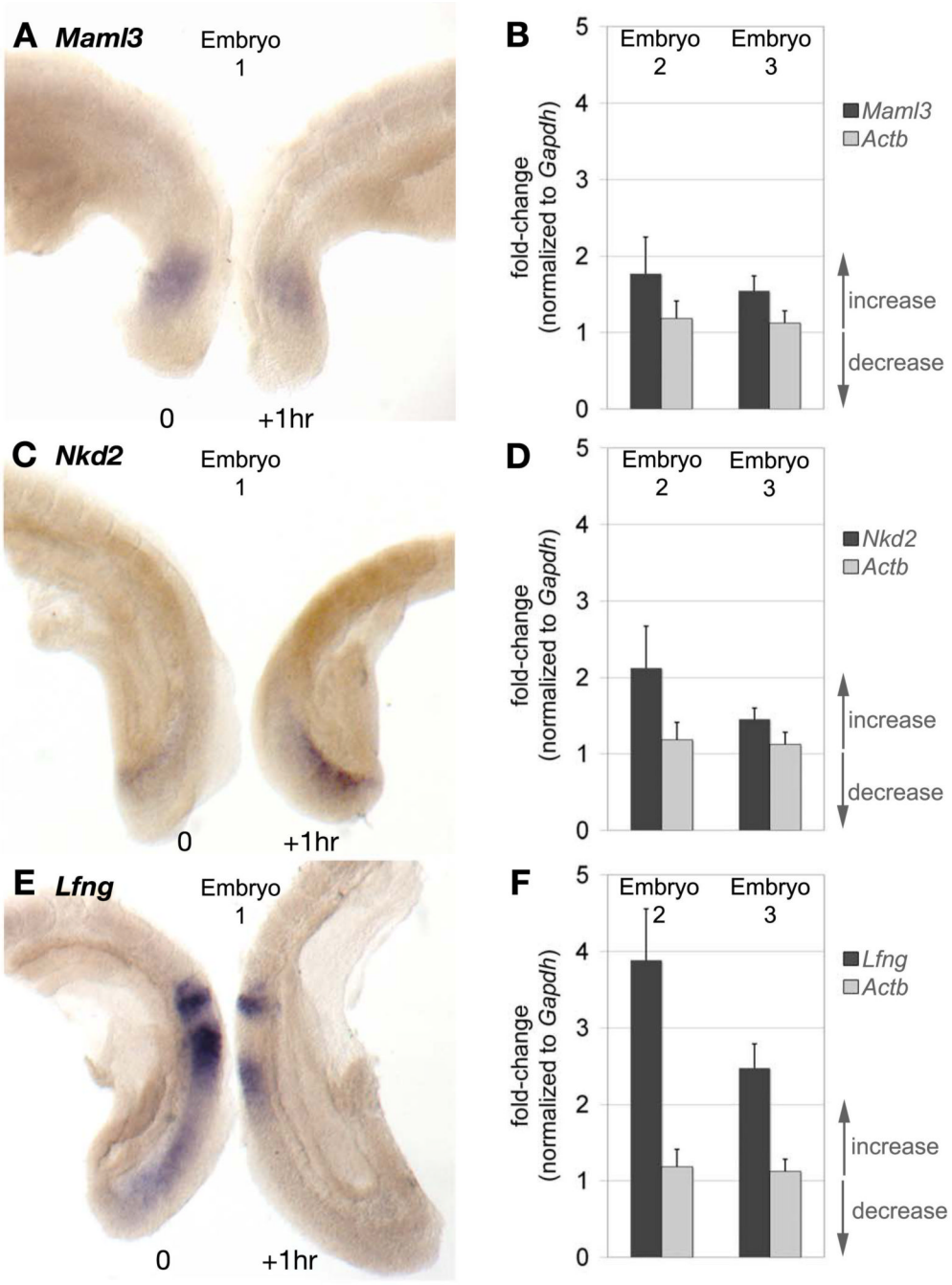

Figure 7.

Expression of *Maml3* (A, B), *Nkd2* (C, D), and *Lfng* (E, F) oscillate in levels as assayed in split embryos analyzed by whole mount *in situ* hybridization (A, C, E) and quantitative PCR (B, D, F). 9.5 dpc embryos were split in half, with the left halves collected immediately and the right halves cultured for 1 hour and then collected for *in situ* analysis or RNA extraction. Three representative embryos are shown for *Maml3*, *Nkd2*, and *Lfng* (Embryo 1 analyzed by RNA *in situ* hybridization and Embryos 2 and 3 by Q-PCR). For Q-PCR analysis from Embryos 2 and 3 (B, D, F), expression values were normalized to *Gapdh* control. For comparison, levels of the housekeeping gene beta-actin (*Actb*) are shown. Levels of *Maml3* were observed to vary in intensity (n=12) by *in situ* hybridization (A), as confirmed by Q-PCR (B). Levels of *Nkd2*

were also observed to vary by *in situ* hybridization (C; n=11), as confirmed by quantitative PCR (D). *Nkd2* levels were measured to display 1.4 and 2.1 fold increase in expression by Q-PCR, whereas *Maml3* displayed less variability (1.5 and 1.8). The cycling gene *Lfng* displayed significant changes in expression by *in situ* hybridization (E), consistent with previous reports (Forsberg et al., 1998;Aulehla et al., 1999), and displayed correspondingly large changes in expression level (2.5 and 3.9, F). By quantitative PCR, we only detected low levels of expression of the other genes present in the PSM, *Glcci1* and *Tcf7l2*, and we did not observe clear evidence of dynamic expression by Q-PCR (data not shown).

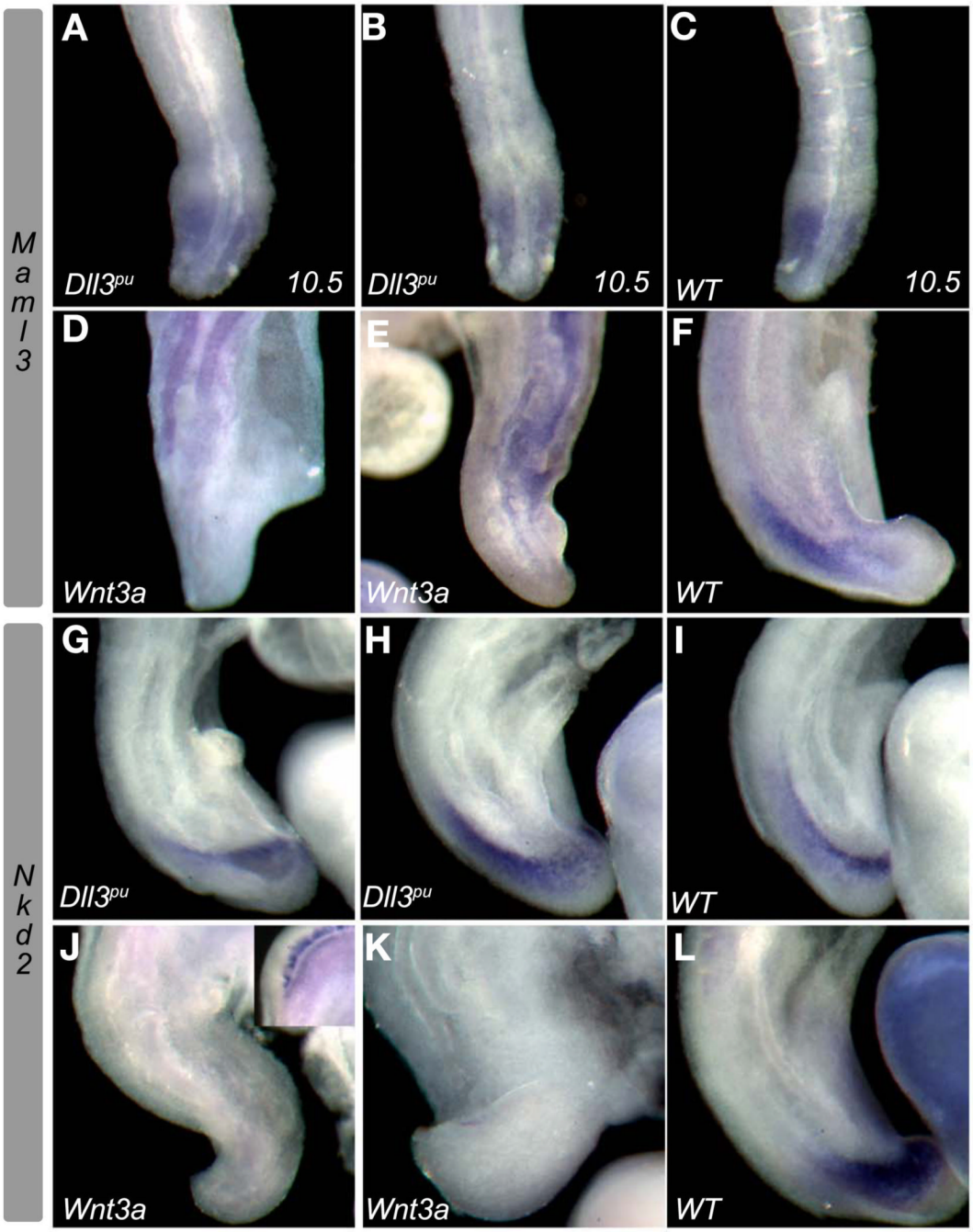

Figure 8.

Expression of *Maml3* and *Nkd2* in $Dll3^{pu}$ and $Wnt3a^{tm1Amc}$ mutant embryos. The $Dll3^{pu}$ mutation has been previously shown to disrupt oscillatory expression of *Lfng* but not *Hes7* (Kusumi et al., 2004), but does not cause the complete loss of gene expression as observed for *Dll1* mutants (Barrantes et al., 1999). All embryos are at 9.5 dpc stage, unless indicated otherwise. Expression of *Maml3* (A-C) is observed in 10.5 dpc $Dll3^{pu/pu}$ embryos (A, B; n=5) at levels comparable to that in wild-type (WT; C) embryos. Variation in *Maml3* levels was observed in $Dll3^{pu}$ mutant embryos, consistent with dynamic expression. In contrast, the more severe PSM disruptions in $Wnt3a^{tm1Amc}$ targeted mutant embryos (D, E; n=5) resulted in a loss of *Maml3* expression compared to wild type embryos (F). For *Nkd2* (G-I), variation in

expression levels is observed in *Dll3*$^{pu/pu}$ embryos (G,H; n=8), consistent with potential oscillatory expression. In contrast, *Nkd2* levels are severely decreased in *Wnt3a* mutant embryos (J, K; n=5) compared to wild-type embryos (L).

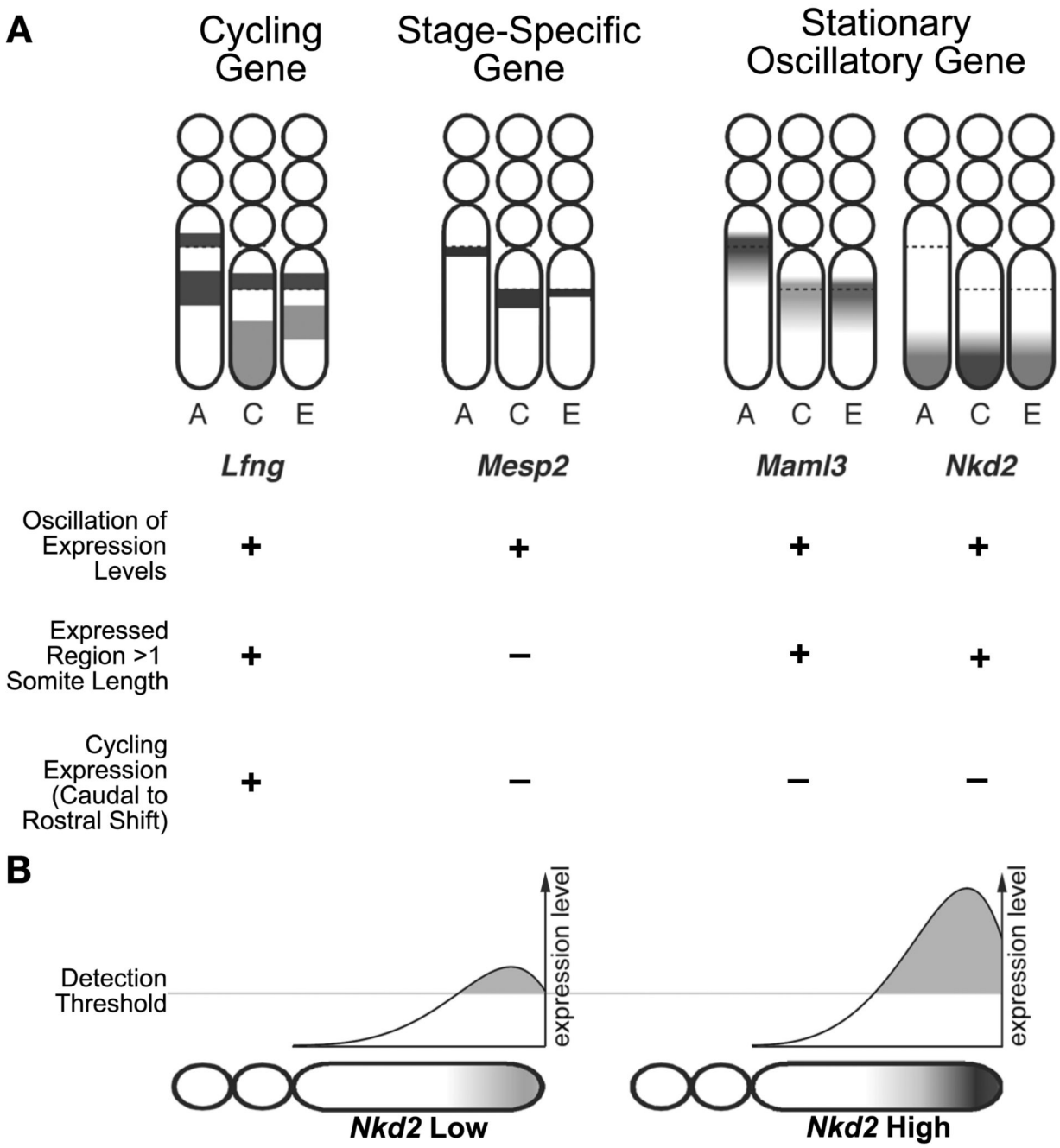

Figure 9.

A, Diagram illustrating oscillatory expression of *Maml3* and *Nkd2* compared to cycling and stage specific genes. Cycling genes such as *Lfng* display caudal to rostral changes in localized expression within the PSM. Stage-specific genes such as *Mesp2* display the stripe of expression with variable length that changes during the somite cycle. Genes such as *Maml3* and *Nkd2* do not fit neatly into either category are in a category of genes with stationary oscillatory expression. Embryos are shown at cycling stages A, C, E (Forsberg et al., 1998). B, Diagram modeling expression of *Nkd2* at the high and low ends of the oscillatory period. While the peak of expression can remain stationary, the expression levels can vary and expression boundaries can display some minor shifts.

Table 1

20 Selected Oscillatory Gene Candidates Identified in Synchronized UCB1 Mesenchymal Stem Cells

Genes with mouse homologues expressed in somites or presomitic mesoderm

Gene	Description	Affymetrix probe ID	Human Q-PCR Assay	Human Unigene	Mouse Unigene	Mouse IMAGE
MAML3	mastermind-like 3	242794_at	Hs00298519_s1	Hs.444627	Mm.331011	6506044
NKD2	naked 2	232201_at	Hs00263909_m1	Hs.240951	Mm.45506	6314370
GLCCI1	glucocorticoid induced gene 1	225706_at	Hs00406849_m1	Hs.131673	Mm.210787	4505211
TCF7L2	transcription factor 7 like 2	212762_s_at	Hs00181036_m1	Hs.214039	Mm.139815	5702449
ID1	inhibitor of DNA binding 1	208937_s_at	Hs00704053_s1	Hs.410900	Mm.444	949768
ID2	inhibitor of DNA binding 2	201566_x_at	Hs00747379_m1	Hs.180919	Mm.34871	6515664

Genes with mouse homologues expressed in non-paraxial mesdermal structures

Gene	Description	Affymetrix probe ID	Human Q-PCR Assay	Human Unigene	Mouse Unigene	Mouse IMAGE
CTGF	connective tissue growth	209101_at	Hs00170014_m1	Hs.410037	Mm.1810	5323271
NUAK1	Ampk related protein kinase 5	204589_at	Hs00934231_m1	Hs.524692	Mm.25874	3662840
SLC2A3	solute carrier family 2A3	202499_s_at	Hs00359840_m1	Hs.419240	Mm.269857	6331145

Genes with mouse homologues without localized expression or below the threshold of detection

Gene	Description	Affymetrix probe ID	Human Q-PCR Assay	Human Unigene	Mouse Unigene	Mouse IMAGE
AMOTL2	angiomotin protein like 2	203002_at	Hs00756906_m1	Hs.426312	Mm.21145	5709126
AXUD1	axin 1 upregulated protein 1	225557_at	Hs01042624_m1	Hs.370950	Mm.125196	5011401
BHLHB2	basic helix-loop-helix B2	201170_s_at	Hs01041212_m1	Hs.171825	Mm.2436	6530971
C14orf43	C14orf43 protein	225980_at	Hs00411442_m1	Hs.509923	Mm.31256	5026104
CYR61	cysteine rich angiogenic	210764_s_at	Hs00155479_m1	Hs.8867	Mm.1231	2616375
HHEX	homeobox protein PRH	204689_at	Hs00242160_m1	Hs.118651	Mm.33896	5124938
KLF10	kruppel-like factor 10	202393_s_at	Hs00194622_m1	Hs.82173	Mm.4292	3155247
RASA4	ras gtpase activing protein 4	212706_at	Hs00419597_g1	Hs.489479	Mm.290655	5361403
SMURF2	smad ubiquitination regulatory factor 2	227489_at	Hs00224203_m1	Hs.515011	Mm.340955	3469700
SNAI2	snail homologue 2	213139_at	Hs00161904_m1	Hs.360174	Mm.4272	466831
ZNF537	zinc finger protein 537	223393_s_at	Hs01583885_m1	Hs.278436	Mm.44141	2865773